Anomalous transitions in two-level systems driven by the ac Stark effect

W. Leo Meerts, Irving Ozier, and Jon T. Hougen

Abstract: An unusual type of nonresonant absorption signal produced by the ac Stark effect has been observed in a two-level avoided-crossing system. The theory for these anomalous transitions has been developed. The nonresonant signals have been shown to be caused by the perturbation by the oscillating field of the dephasing of the two-level system at the avoided crossing. A series of measurements of these anomalous transitions has been carried out using the avoided-crossing molecular-beam electric-resonance technique. In addition, different types of resonant multiphoton transitions have been investigated. Results are reported for the AE-barrier anticrossing with $J = 1$ in CH_3SiH_3. The experimental findings are in good agreement with the theory developed.

PACS Nos.: 33.20Bx, 33.80Be, 42.50Hz

Résumé: Nous observons un type inhabituel d'absorption non résonante produite par un effet Stark ac dans un système à deux niveaux évitant le croisement. Nous développons une théorie décrivant ces transitions anomales. Nous montrons que les signaux de non-résonance résultent de la perturbation causée par le décalage du système à deux niveaux lors de l'évitement du croisement. Nous avons effectué des séries de mesures sur ces transitions anomales en utilisant la technique de résonance électrique dans un faisceau moléculaire. Nous analysons aussi différents types de transitions résonantes multiphoniques. Nous présentons des résultats pour une barrière anticroisement AE avec $J = 1$ dans du CH_3SiH_3. Les résultats expérimentaux sont en bon accord avec ceux de la théorie développée ici.

[Traduit par la Rédaction]

1. Introduction

In the understanding of the interactions between radiation and matter, the two-level problem [1] plays a fundamental role. A two-level problem is defined as a system in which two individual states have interactions only with each other and with external fields. Avoided crossings in symmetric top

Received July 20, 2000. Accepted November 23, 2000. Published on the NRC Research Press Web site on May 2, 2001.

W.L. Meerts.[1] Department of Molecular and Laser Physics, University of Nijmegen, P.O. Box 9010, 6500 GL Nijmegen, The Netherlands.
I. Ozier. Department of Physics and Astronomy, University of British Columbia, 6224 Agricultural Road, Vancouver, BC V6T 1Z1, Canada.
J.T. Hougen. Optical Technology Division, National Institute of Standards and Technology, Gaitherburg, MD 20899-8441, U.S.A.

[1] Corresponding author Telephone: +31 24 365 3023; FAX: +31 24 365 3311; e-mail: Leo.Meerts@sci.kun.nl

 DOI: 10.1139/cjp-79-2/3-533

molecules were found to provide an ideal example of an isolated two-level system, and can be used to study the behaviour of this system in external oscillating fields. In a previous paper [2], an unusual type of resonant multiphoton transition was reported. Absorption of as many as 40 photons was detected under moderate conditions. To drive these transitions, the amplitude of the monochromatic oscillating field was only a factor 40 larger than was needed to optimize the corresponding one-photon transition. It was found that the linear ac Stark effect was responsible for this effect. In particular, as a result of the K-degeneracy that exists for $K \neq 0$ in a symmetric top, the Stark effect produces diagonal terms in the two-by-two Hamiltonian matrix for the two-level system. These diagonal Stark terms can be transformed into the more usual off-diagonal position in the matrix, but now associated with an effective oscillating field which contains a large number of harmonics of the single frequency being applied. Measurements were taken in a fixed static electric field by sweeping the frequency of the oscillating field.

Two-photon microwave transitions associated with the same mechanism have been observed by Martinache et al. [3]. In that experiment, the frequency of the oscillating field was approximately 8.6 GHz. The two-photon transitions were detected by observing one-photon emission signals at 17.3 GHz with a Fourier transform crossed-cavity spectrometer. The identification of the absorption mechanism was confirmed by showing that only the transitions with $K \neq 0$ appeared in the spectrum when the radiation was properly filtered, even though the ($K = 0$) lines were easily observed when the filtering was removed. This experiment clearly demonstrated that the multiphoton transitions are not limited to the avoided-crossing technique or to the radio-frequency region, but are of a much more general nature.

Several studies of multiphoton transitions in a two-level system have been discussed in the literature in a variety of other fields, including magnetic resonance [4] and multiphoton excitation with intense laser pulses [5]. Perhaps the most relevant of these related studies is the work on multiphoton microwave transitions between Rydberg states in potassium [6, 7]. These Rydberg studies involve pairs of levels that undergo an avoided crossing, with at least one of the interacting levels having a linear Stark effect. Although the system being investigated, the experimental methods, and the theoretical treatment are all rather different from those in our earlier work [2], the underlying physics is very similar in the two cases. The theoretical approach used in the current paper will be modelled on that developed in our earlier investigation of multiphoton transitions in symmetric rotors [2].

During a series of molecular-beam electric-resonance (MBER) studies on avoided crossings [8–11], another type of anomalous transition was observed. The crossing field for an anticrossing is defined to be the value of the constant external electric field for which the energy separation between the two interacting levels is a minimum. At (or near) the crossing field, transitions between the two levels could be driven with a monochromatic electric field oscillating at a frequency that was arbitrary (within very broad limits). The fixed-energy separation of the two levels was typically of the order of a few kHz, while the frequency of the oscillating field was varied typically from 50 to 1000 kHz. The associated signals are clearly nonresonant. These nonresonant transitions played a very important role in the avoided-crossing studies [8–11]. Since the strength of these anomalous absorption signals was insensitive to the frequency of the oscillating field, these signals were extremely useful in making an initial determination of the crossing field for two levels whose zero-field energy separation was poorly known beforehand.

In the current paper, the theory is developed that is needed to describe these anomalous nonresonant transitions. It is shown that the absorption arises from the perturbation by the oscillatory field of the dephasing of the two-level system at the crossing. As was the case with the resonant multiphoton transitions reported earlier [2], the absorption mechanism for these nonresonant transitions requires that at least one of the two levels has a linear Stark effect. A series of measurements has been carried out with the constant field set to the crossing value to within experimental error. Good agreement was found between the experimental observations and the theoretical predictions. Besides these avoided-crossing MBER measurements at the crossing, further studies of the resonant multiphoton process have been carried out, including one in which the frequency of the oscillating field is held fixed and the static field is varied. In each such study, the dependence of the transition probability on the strength of the

radio-frequency field is investigated. In each case, it is found that the theoretical predictions are in good agreement with the experimental data.

2. Theory

2.1. Background

The analysis starts with the basic equations of an anticrossing system of two levels $j = 1$ or 2, as discussed in detail in ref. 8. The levels are tuned to the avoided crossing by the application of a constant homogeneous external electric field ξ.[2] However, the limit $\xi \to 0$ will be considered first. In this limit, three assumptions are made. First, it is assumed that each of the two levels has a linear dependence of its energy on the field.[3] Second, it is assumed that the dipole-moment operator μ does not couple the two states, except possibly through higher order terms, which will be neglected. Third, it is assumed that the Stark effect is positive for the lower level ($j = 1$) and negative for the upper level ($j = 2$). Under these conditions, as ξ is increased from zero, it will eventually reach a value at which the Stark effect cancels the zero-field energy splitting Δ_0, which is here defined so as to be positive. This value of ξ is the crossing field ξ_C (defined above), and the levels will cross at this field if no additional interaction is present. However, if there exists a nonzero coupling matrix element between the two states, they will undergo an avoided crossing. This coupling matrix element can arise from a variety of different mechanisms. For symmetric tops, a number of these mechanisms have been discussed in refs. 8,9,11–13. The magnitude of the coupling matrix element will here be denoted $\frac{1}{2}\hbar\omega_c$. (The sign does not affect any of the results obtained in the current work.) When $\hbar\omega_c$ is smaller than the instrumental resolution, it has not been possible to determine this coupling matrix element by direct frequency measurements.

The specific case studied in the current work[4] is the AE-barrier avoided crossing ($J = 1, K = \mp 1, \sigma = 0, m_J = \pm 1, \Gamma = E_1$) $\longleftrightarrow$ ($1, \pm 1, \mp 1, \pm 1, E_3$) in CH_3SiH_3 [9]. See, in particular, the energy level diagram shown in Fig. 2 of ref. 9. In the limit $\xi \to 0$, the ($\Gamma = E_1$) state is the lower level, here labelled ($j = 1$), while the ($\Gamma = E_3$) state is the upper level, here labelled ($j = 2$). The crossing field in this case is $\xi_C = 1.719$ kV/cm. The diagonal electric dipole matrix element $\mu_{jj} = \mu(J, K, m_J) = \mu K m_J / J(J + 1)$, where the permanent dipole moment $\mu = 0.734\,560(3)$ D (1 D = $3.335\,64 \times 10^{-30}$ C m) [14]. For this particular anticrossing, $\mu_{22} = -\mu_{11} = \mu/2$.

2.2. Time evolution of a two-level system without an external excitation field

The Hamiltonian $\tilde{H}$ for the two-level anticrossing system will initially be investigated in the absence of an external oscillating field. In this case, $\tilde{H}$ has no explicit time-dependence and can be written as the sum of two time-independent parts: H_0, which describes the zero-field splitting and the linear Stark effect, and H_c, which describes the coupling between the two levels.

$$\tilde{H} = H_0 + H_c \tag{1}$$

For H_0, the eigenvalues and time-dependent eigenfunctions are written $E_j^{(0)}$ and $\Psi_j(t)$, respectively,

[2] The results obtained here for the electric field case can be easily converted to the form appropriate to the corresponding magnetic case.

[3] The present analysis can easily be adapted to the case where only one of the two levels has a linear Stark effect.

[4] In the specification of the quantum numbers for the avoided crossing, upper signs go with upper, and lower signs with lower. The system of levels can be thought of as consisting of two independent two-level problems. In fact, when the nuclear spin quantum numbers are taken into account, there are many more levels involved. It has been shown that these break up into a series of two-level problems if a small magnetic field is applied; see refs. 8 and 13. In the current work, the data were taken in the ambient magnetic field, and the break-up into a series of two-level problems is based on empirical evidence, as was the case in ref. 13.

with $j = 1, 2$. The Hamiltonian matrix for H_0 can be written

$$(H_0) = \begin{pmatrix} E_1^{(0)} & 0 \\ 0 & E_2^{(0)} \end{pmatrix} = \begin{pmatrix} -\frac{1}{2}\Delta_0 - \mu_{11}\xi & 0 \\ 0 & +\frac{1}{2}\Delta_0 - \mu_{22}\xi \end{pmatrix} \tag{2}$$

So that the signs of the linear Stark effects lead to an avoided crossing (as noted above), it is required that $\mu_{11} < 0$ and $\mu_{22} > 0$. As can be seen from Sect. 2.1, the AE-barrier avoided crossing of interest here meets this requirement. The second-order Stark effect is neglected here. The symbol $\hbar\omega_0$ will be used to represent the energy difference $(E_2^{(0)} - E_1^{(0)})$.[5] Here $\hbar\omega_0$ is positive below the crossing, zero at the crossing ($\xi = \xi_C$), and negative above. The time-dependent eigenfunctions of H_0 can be written in the standard manner in terms of the time-independent spatial eigenfunctions $\psi_j(\boldsymbol{r})$

$$\Psi_j(t) = \psi_j(\boldsymbol{r})\, \mathrm{e}^{-iE_j^{(0)}t/\hbar}, \qquad H_0\psi_j(\boldsymbol{r}) = E_j^{(0)}\psi_j(\boldsymbol{r}) \tag{3}$$

In the basis $\{\psi_1(\boldsymbol{r}), \psi_2(\boldsymbol{r})\}$, the matrix for $\tilde{H}$ itself can be written

$$\left(\tilde{H}\right) = \begin{pmatrix} E_1^{(0)} & 0 \\ 0 & E_2^{(0)} \end{pmatrix} + \begin{pmatrix} 0 & \frac{1}{2}\hbar\omega_c \\ \frac{1}{2}\hbar\omega_c & 0 \end{pmatrix} \tag{4}$$

For $\tilde{H}$, the eigenvalues are written E_j, with $j = 1, 2$. The choice for the labels 1 and 2 is made such that the energy difference $(E_2 - E_1)$ between the two states is positive below the crossing and negative above. (This choice is in accordance with that made earlier for $(E_2^{(0)} - E_1^{(0)})$.) From (4), $|E_2 - E_1| = \hbar\omega_{res} = \sqrt{(E_2^{(0)} - E_1^{(0)})^2 + (\hbar\omega_c)^2}$, where ω_{res} is the associated resonance frequency. Far from the avoided crossing, $|E_2 - E_1| \simeq \left|E_2^{(0)} - E_1^{(0)}\right| \gg \hbar\omega_c$, and the effect of H_c on the energies E_j can be neglected. At the crossing field, $|E_2 - E_1|$ takes the value $\hbar\omega_c$. Near the avoided crossing, not only are the energies affected by H_c, but, in addition, the time evolution of the eigenfunctions is affected, *even* in the absence of an explicit time-dependence in $\tilde{H}$. This is caused by the mixing of the states $\{\psi_1(\boldsymbol{r}), \psi_2(\boldsymbol{r})\}$ by the off-diagonal terms in H_c. In effect, the system is prepared with ξ far from ξ_C in an eigenstate of H_0, which is not an eigenstate of $\tilde{H}$. Then $|\xi - \xi_C|$ is reduced to zero and, as is shown below, the system oscillates between the eigenstates of H_0.

The time-dependent solution $\widetilde{\Phi}(t)$ of the complete Hamiltonian $\tilde{H}$ can be obtained in the form

$$\widetilde{\Phi}(t) = \tilde{a}_1(t)\Psi_1(t) + \tilde{a}_2(t)\Psi_2(t) \tag{5}$$

By substituting (5) into $\tilde{H}\widetilde{\Phi}(t) = i\hbar(\partial\widetilde{\Phi}(t)/\partial t)$, multiplying by Ψ_j^*, and integrating over the spatial variables, the following pair of differential equations are obtained for $\tilde{a}_1(t)$ and $\tilde{a}_2(t)$:

$$i\hbar\frac{\mathrm{d}\tilde{a}_1(t)}{\mathrm{d}t} = \frac{1}{2}\hbar\omega_c\tilde{a}_2(t)\,\mathrm{e}^{-i\omega_0 t}, \qquad i\hbar\frac{\mathrm{d}\tilde{a}_2(t)}{\mathrm{d}t} = \frac{1}{2}\hbar\omega_c\tilde{a}_1(t)\,\mathrm{e}^{+i\omega_0 t} \tag{6}$$

Equations (6) can be solved analytically. It will be assumed that all molecules are in state $j = 1$ before entering the region where ξ is close to ξ_C, and stay in that region for a time t. The initial conditions then are $\tilde{a}_1(t = 0) = 1$, and $\tilde{a}_2(t = 0) = 0$. With these initial conditions, the solution for $\tilde{a}_1(t)$ can be written

$$\tilde{a}_1(t) = \mathrm{e}^{-i\omega_0 t/2}\left[\cos\left(\frac{1}{2}\tilde{\Omega}t\right) + i\frac{\omega_0}{\tilde{\Omega}}\sin\left(\frac{1}{2}\tilde{\Omega}t\right)\right], \qquad \tilde{\Omega} = \sqrt{\omega_0^2 + \omega_c^2} \tag{7}$$

[5] It should be noted that the definition of ω_0 used in the current paper differs slightly from the one used in ref. 2.

The probability of finding the molecule in state $j = 1$ is given by $|\tilde{a}_1(t)|^2$. Consequently, the change $(\Delta\tilde{I})$ in the number of molecules in state $j = 1$ after the molecules have been in the region near the avoided crossing for a time t is $|\tilde{a}_1(t)|^2 - |\tilde{a}_1(0)|^2$, where

$$\Delta\tilde{I} = |\tilde{a}_1(t)|^2 - 1 = -\frac{\omega_c^2}{\tilde{\Omega}^2}\sin^2\left(\frac{1}{2}\tilde{\Omega}t\right) \tag{8}$$

2.3. The effects of a time-dependent resonant field far from the crossing

The effect on the two-level system will now be investigated of a coherent excitation field of the form $V(t) = \varepsilon\cos\omega t$. Here ε and ω are, respectively, the electric field strength and the angular frequency of the applied radio-frequency field. Approximations will be made that are appropriate to the case where $|\xi - \xi_C|$ is large and (ω/ω_0) is close to (or equal to) an integer value. These conditions correspond, respectively, to being far from the crossing and to being near (or on) resonance. The Hamiltonian H describing this system is given by

$$H = H_0 + H_c + V(t) \tag{9}$$

In the basis $\{\psi_1(\boldsymbol{r}), \psi_2(\boldsymbol{r})\}$, the matrix for Hamiltonian H can be written

$$(H) = \begin{pmatrix} E_1^{(0)} & 0 \\ 0 & E_2^{(0)} \end{pmatrix} + \begin{pmatrix} 0 & \frac{1}{2}\hbar\omega_c \\ \frac{1}{2}\hbar\omega_c & 0 \end{pmatrix} + \begin{pmatrix} -\mu_{11}\varepsilon\cos\omega t & 0 \\ 0 & -\mu_{22}\varepsilon\cos\omega t \end{pmatrix} \tag{10}$$

The time-dependent solution $\Phi(t)$ of H can be written as a linear superposition of the two functions $\Psi_j(t)$ $(j = 1, 2)$ as in (5), but with new superposition constants $a_j(t)$. By following the procedure used to derive (6), the following pair of differential equations can be obtained for the $a_j(t)$:

$$\begin{aligned} i\hbar\frac{da_1(t)}{dt} &= -\mu_{11}\varepsilon\cos\omega t\ a_1(t) + \frac{1}{2}\hbar\omega_c a_2(t)\,e^{-i\omega_0 t} \\ i\hbar\frac{da_2(t)}{dt} &= +\frac{1}{2}\hbar\omega_c a_1(t)\,e^{+i\omega_0 t} - \mu_{22}\varepsilon\cos\omega t\ a_2(t) \end{aligned} \tag{11}$$

The case currently under consideration where the static external field ξ is far from the crossing value ξ_C was treated in our earlier work [2]. It was found that the effect of $V(t)$ on the diagonal in (10) could be transformed to the more usual off-diagonal position in the matrix through the introduction of an *effective* oscillating field, which contains a large number of harmonics of the frequency ω actually being applied. The nth harmonic can induce multiphoton transitions when the resonance condition $n\omega \approx \omega_0$ is met. In this case, the change (ΔI) in the number of molecules in state $j = 1$ after the molecules have been in the C-field region for a time t is

$$\Delta I = |a_1(t)|^2 - 1 = -\frac{x_n^2}{\Omega_n^2}\sin^2\left(\frac{1}{2}\Omega_n t\right)$$

where

$$\Omega_n = \sqrt{(n\omega - \omega_0)^2 + x_n^2}$$

and

$$x_n = \omega_c J_n\left[\frac{(\mu_{22} - \mu_{11})\,\varepsilon}{\hbar\omega}\right] \tag{12}$$

Here J_n is the Bessel function [16] of integer order n with $|n| \geqslant 1$. As was done in Sect. 2.2 for $\widetilde{a}_j(t)$, the initial conditions applied to $a_j(t)$ were $a_1(t = 0) = 1$; $a_2(t = 0) = 0$. Note that the expression for ΔI given in (12) for the situation being considered here has the same form as that given in (8) for the situation considered in Sect. 2.2.

2.4. The effects of a time-dependent nonresonant field at the crossing

The case of primary interest in the current work where $\omega_{\text{res}} \approx \omega_{\text{c}}$ and $\omega \gg \omega_{\text{res}}$ will now be investigated. These conditions correspond, respectively, to the static external field ξ being close to the crossing value ξ_{C}, and to the frequency of the oscillating field being far above the resonance value. Much of the previous development still applies. The Hamiltonian H of (10) is valid. The time-dependent solution $\Phi'(t)$ of H must satisfy (5) with superposition constants $a'_j(t)$, but the primes have been added to indicate explicitly that the solution is qualitatively different from that discussed in Sect. 2.3. The $a'_j(t)$ satisfy (11), but different approximations will be introduced.

The physical problem now being considered is quite different from those previously discussed in the literature. In particular, it is quite different from the usual two-level problem discussed by Shimoda [15], and from the problem of the multiphoton transitions described in Sect. 2.3. In both the former and the latter, the rotating-wave approximation is made; while, in the latter, a near-resonance assumption is made that the angular frequency ω of the applied oscillating field or its nth harmonic $n\omega$ is close (or equal) to $|E_2 - E_1|/\hbar$. In the problem considered in the current section, both the rotating wave and its counter-rotating partner are off-resonance by about the same frequency difference since $\omega \gg \omega_{\text{res}}$. In spite of this, because $\omega_0 = 0$, a single assumption can be introduced that is equivalent to the rotating wave approximation and the near-resonance assumption combined.

To solve (11) for the $a'_j(t)$, the substitution given in eq. (7) of ref. 2 is made,

$$a'_j(t) = \mathrm{e}^{i(\mu_{jj}\varepsilon/\hbar\omega)\sin\omega t} X_j(t) \tag{13}$$

Then a Fourier expansion of $\mathrm{e}^{i[(\mu_{22}-\mu_{11})\varepsilon/\hbar\omega]\sin\omega t}$ is carried out. This yields

$$\begin{aligned} i\hbar\frac{\mathrm{d}X_1(t)}{\mathrm{d}t} &= \frac{1}{2}\hbar\omega_{\text{c}}\sum_{n=-\infty}^{+\infty} J_n\left[\frac{(\mu_{22}-\mu_{11})\varepsilon}{\hbar\omega}\right]\mathrm{e}^{+in\omega t}\,\mathrm{e}^{-i\omega_0 t}X_2(t) \\ i\hbar\frac{\mathrm{d}X_2(t)}{\mathrm{d}t} &= \frac{1}{2}\hbar\omega_{\text{c}}\sum_{n=-\infty}^{+\infty} J_n\left[\frac{(\mu_{22}-\mu_{11})\varepsilon}{\hbar\omega}\right]\mathrm{e}^{-in\omega t}\,\mathrm{e}^{+i\omega_0 t}X_1(t) \end{aligned} \tag{14}$$

It is now assumed that ω_0 vanishes.[6] This simplifying assumption is justified by the fact that the experimental data were taken with $|\xi - \xi_{\text{C}}| = 0$ (to within experimental error). It is then noted that the analog of resonance occurs for this case when $n\omega = \omega_0 = 0$, i.e., when $n = 0$. Since n specifies the harmonic of the effective applied radio-frequency field that results from the substitution made in (13), the $(n = 0)$ case corresponds to the resonance being driven by the D.C. component of this effective field. The assumption will be made that only this $(n = 0)$ component is important to the time evolution of $X_1(t)$ and $X_2(t)$. This *D.C. assumption* is equivalent to the combination of the rotating-wave approximation and the near-resonance approximation because, when $n = 0$, the value of ω is irrelevant (within very broad limits). Once the D.C. assumption is made, (14) becomes

$$\begin{aligned} i\hbar\frac{\mathrm{d}X_1(t)}{\mathrm{d}t} &= \frac{1}{2}\hbar\omega_{\text{c}}J_0\left[\frac{(\mu_{22}-\mu_{11})\varepsilon}{\hbar\omega}\right]X_2(t) \\ i\hbar\frac{\mathrm{d}X_2(t)}{\mathrm{d}t} &= \frac{1}{2}\hbar\omega_{\text{c}}J_0\left[\frac{(\mu_{22}-\mu_{11})\varepsilon}{\hbar\omega}\right]X_1(t) \end{aligned} \tag{15}$$

The differential equations (15) have the exact solution

$$X_1(t) = \cos\left(\omega_{\text{c}}J_0\left[\frac{(\mu_{22}-\mu_{11})\varepsilon}{\hbar\omega}\right]\frac{t}{2}\right) \tag{16}$$

[6] Of course, ω_{c} was not set equal to zero.

Fig. 1. Comparison between the numerical solution of (14) and the analytical solution given in the second equation of (17). The former was used to generate the open dots, while the latter was used to generate the line.

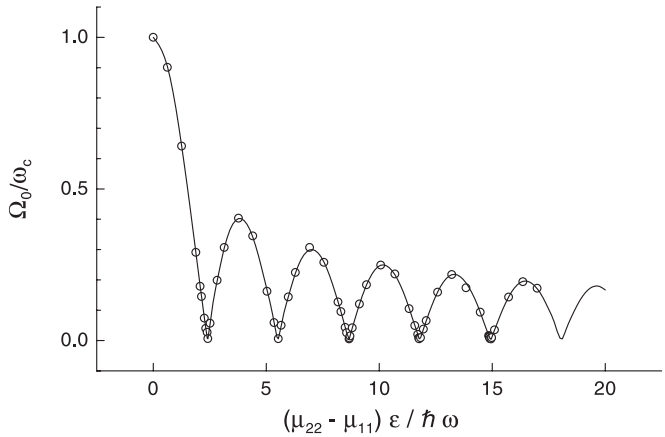

so that

$$\left|a_1'(t)\right|^2 = \cos^2\left(\frac{1}{2}\Omega_0 t\right), \qquad \Omega_0 = \omega_c J_0\left[\frac{(\mu_{22} - \mu_{11})\,\varepsilon}{\hbar\omega}\right] \tag{17}$$

Here J_0 is the Bessel function [16] of order 0. It is interesting to note that the expression for Ω_n obtained from (12) has the same form as that for Ω_0 in the current case where the frequency ω is far above resonance.

The accuracy of the analytical solution given in (17) is illustrated in Fig. 1 by making a comparison with the numerical solution of (14). To characterize the analytical solution for $\left|a_1'(t)\right|^2$, the value of (Ω_0/ω_c) was calculated with the second equation of (17). To characterize the numerical solution, (Ω_0/ω_c) was calculated with Ω_0 obtained from the first equation of (17) using the numerically determined value of $\left|a_1'(t)\right|^2$. To generate Fig. 1, the comparison was made for various different sets of values for t, ω_c, ω, and ε covering the range relevant for the current experiment. From Fig. 1, it is clear that the analytical solution and the numerical calculations agree very well indeed.

3. Experimental details and results

3.1. Background

The basic molecular beam electric resonance (MBER) apparatus has been described in detail elsewhere [17, 18]. The experimental methods and conditions were very similar to those used before for CH_3SiH_3 [9,14]. The sample was made by reducing CH_3SiCl_3 with $LiAlH_4$. The data were taken using the ion peak with a mass-to-charge ratio of 44. The seeded-beam technique was used; a 5% mixture of methyl silane in argon at a backing pressure between 1 and 1.5 bar (1 bar = 10^5 Pa) was expanded through a 50 μm nozzle with the source at room temperature. The velocity v of the molecules in the beam was ∼550 m/s and the rotational temperature was ∼5 K. The measurements were taken in the ambient magnetic field.

The static and oscillating electric fields in the transition region were generated by the Pyrex C-field described in ref. 19. See, in particular, the coating pattern of the plates shown in Fig. 1 of ref. 19. For the anticrossing measurements, it was necessary to observe only transitions with $\Delta m_T = 0$, where m_T is the eigenvalue of the component along $\boldsymbol{\xi}$ of the total angular momentum. Consequently, the C-field was connected in the parallel plate configuration with $\boldsymbol{\xi}$ and $\boldsymbol{\varepsilon}$ parallel. Four different sections with lengths along the molecular beam of 2.2, 3.6, 2.1, and 2.0 cm were available. The wires connecting to these

Fig. 2. Free-decay intensity as a function of the length l of the C-field. The solid triangles are the measurements, while the line represents the best fit to the experimental data using (8).

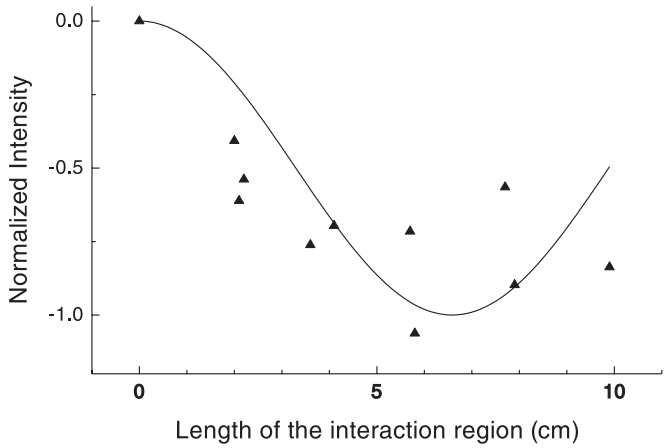

sections were accessible from outside the vacuum. Using these wires, the four sections were divided into an *active region* to which the oscillating field $\boldsymbol{\varepsilon}$ was applied when necessary, and an *inactive region* to which $\boldsymbol{\varepsilon}$ was not applied. The active region (of length l) consisted of either a single section, or a set of contiguous sections. The static field on the inactive region was sufficiently different from that on the active region that the inactive region did not have to be taken into account in analyzing the data. In this way, the effective interaction time $\tau = l/v$ in the avoided-crossing region could be varied.

3.2. Free decay of the molecular state

The first experiment was carried out with the static electric field set to the crossing value ($\xi = \xi_C$, $\omega_0 = 0$), and with no oscillatory exciting field present. This is the situation considered in Sect. 2.2. The molecules enter the C-field[7] after being state-selected by the A-focussing field in the level that has a positive Stark effect. In the notation of Sect. 2.2, all molecules enter the avoided-crossing region in state ($j = 1$); that is, $\tilde{a}_1(t = 0) = 1$. The B-focussing field operates as an analyzer, defocussing molecules in levels with a negative Stark effect. Consequently, molecules leaving the C-field in the ($j = 2$) state are removed from the beam, and the signal $\Delta\tilde{I}$ at the detector is given by (8) with $t = \tau = l/v$. In practice, the experiment was carried out by first measuring the intensity with $\xi = \xi_C$ and then subtracting the corresponding intensity measured with the static electric field ξ switched to a value far enough away from ξ_C that no transitions occur as the molecular beam passed through the C-field. Note that $\Delta\tilde{I} < 0$, since a decrease in signal occurs when $\xi = \xi_C$.

The signal $\Delta\tilde{I}$ was measured for a number of lengths l of the C-field. The observed points were fit to (8) with $v = 550$ m/s and $\omega_0 = 0$. The only adjustable parameters in the fit were $\nu_c = \omega_c/2\pi$ and the signal normalization. The best fit to the experimental data was obtained for $\nu_c = 4.2(1.0)$ kHz.[8] The experimental measurements and the best calculated fit are compared in Fig. 2. In assessing this comparison, it must be remembered that accurate measurements of intensity in an MBER experiment under these conditions are quite difficult, since the accuracy depends on various experimental conditions, such as inhomogeneities in the static electric field, which can change with the length of the C-field. The agreement in Fig. 2 is consequently regarded as satisfactory, a conclusion supported by the fact that the value obtained for ν_c agrees quite well with the more accurate result determined in Sect. 3.3.

[7] It is understood from the context that the term "C-field" refers here only to the active region.

[8] Uncertainties given in parentheses here and elsewhere for ν_c are of Type A and represent one standard uncertainty for this parameter, as obtained from the various least-squares fits to experimental data described in the text.

Fig. 3. Normalized intensity of the resonant single-photon transition as a function of the amplitude ε of the oscillating field: (*a*) $\nu = \nu_0 = 100$ kHz; (*b*) $\nu = \nu_0 = 200$ kHz. The solid symbols are the experimental data. The lines were obtained by fitting the data to (12).

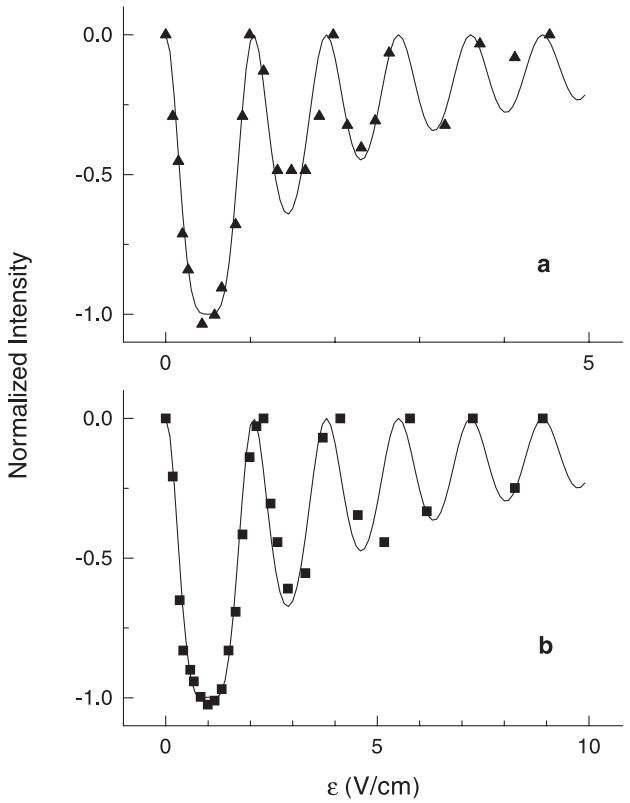

3.3. Analysis of multiphoton transitions

In our earlier work [2], a series of measurements on OPF_3 and CH_3CF_3 was presented for the values of ε at which $\sin^2\left(\frac{1}{2}\Omega_n\tau\right)$ in (12) reaches its *first* maximum.[9] In ref. 2, the value ε associated with this *first* maximum was denoted $E_{\text{opt}}^{(n)}$. See, in particular, column 6 of Tables I and II of ref. 2. These measurements were done for various values of the number n of absorbed photons. They led to values of ν_c for the anticrossings studied.

Similar measurements were made here for $n = 1$ for the avoided crossing being studied in CH_3SiH_3, in part to determine ν_c by another method. In the current work, the frequency $\nu = \omega/2\pi$ of the oscillating field was set to 100 kHz and the static field ξ was used to tune the energy level spacing to resonance for the one-photon transition. With ξ and ν fixed, the signal ΔI was measured as a function of the amplitude ε of the oscillating field. The experiment was then repeated with $\nu = 200$ kHz. The results are presented in Fig. 3*a* for $\nu = 100$ kHz and in Fig. 3*b* for $\nu = 200$ kHz. Several maxima were observed in each case.

The results for each value of ν were fit to (12). The dipole parameter $(\mu_{22} - \mu_{11}) = \mu$; see Sect. 2.1. Thus, the only adjustable parameters again were ν_c and the signal normalization. As can be seen from Fig. 3, the agreement was very good for each value of ν. In assessing the quality of the fits, it

[9] For most of the cases investigated here, the first maximum in the transition probablity at the resonance ($n\omega = \omega_0$) occurs at the value of ε for which $J_n\left[(\mu_{22} - \mu_{11})\,\varepsilon/\hbar\omega\right]$ reaches *its* first maximum.

Fig. 4. Relative intensity as a function of the difference $(\xi - \xi_C)$ between the applied static electric field ξ and the field value ξ_C at the crossing: (*a*) the amplitude ε of the oscillating field = 3.7 V/cm; (*b*) $\varepsilon = 1.7$ V/cm. The downward-pointing peaks (negative signals) arise from the n-photon resonant transitions, while the upward-pointing peak (positive signal) arises from the perturbation of the dephasing at ξ_C. In (*a*), transitions for n as high as 15 can be seen on each side of the crossing.

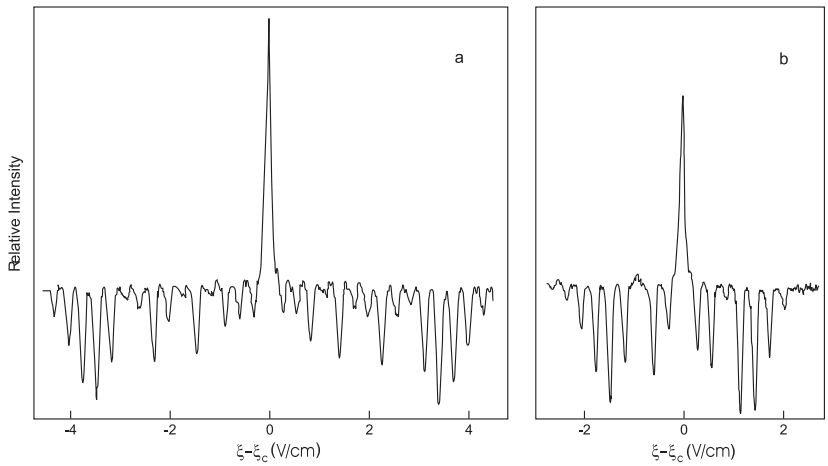

must be recognized that, for the case described by (12), the positions of the maxima in the plots of Fig. 3 are insensitive to ν_c and are determinded only by the Bessel function $J_1[(\mu_{22} - \mu_{11})\,\varepsilon/\hbar\omega]$, whose argument has no adjustable parameters. The agreement for the positions of the first three maxima in Figs. 3*a* and 3*b* is particularly satisfying.

The best fit values for ν_c were 4.7(6) kHz for $\nu = 100$ kHz and 4.9(6) kHz for $\nu = 200$ kHz; the average value is 4.8(5) kHz. It was found empirically that the depth of the modulation in the plots of Fig. 3 is determined by $\nu_c l/v$. In the fits shown here, it was assumed that all the molecules had the same velocity v of ~550 m/s. However, the typical spread in the molecular velocities is about 10%. This spread produces a damping of the modulation depth, so that the best fit value obtained here for ν_c is a little too small. In spite of this, the agreement with the value of ν_c obtained in Sect. 3.2 is good.

A different type of study was carried out in which the angular frequency ω and amplitude ε of the oscillating field were kept fixed, while the static field ξ was scanned through the region of the crossing value ξ_C. It is scans of this type that were used to make preliminary searches for anticrossings, as discussed in Sect. 1. In such a scan, the n-photon resonance condition discussed in Sect. 2.3 was met for many values of n on both sides of the crossing. This can be seen in Fig. 4. The downward-pointing peaks (negative signals) are produced by n-photon resonant transitions, while the very strong upward-pointing peak (positive signal) arises from the perturbation of the dephasing at ξ_C to be discussed in Sect. 3.4. The data were taken with $\varepsilon = 3.7$ and 1.7 V/cm in panels (*a*) and (*b*), respectively, of Fig. 4. In both cases, $\nu = 100$ kHz and $l = 10$ cm. As in the other studies, $v = 550$ m/s. The spacing between the peaks should be approximately constant, and the curves should be symmetric about $\xi = \xi_C$. The peak intensities of the various n-photon transitions were fit to (12); the only adjustable parameters were again ν_c and the signal normalization. A good fit was obtained. The best fit values for ν_c were 5.2(5) kHz and 5.6(9) kHz for $\varepsilon = 3.7$ and 1.7 V/cm, respectively. The weighted mean of 5.3(4) kHz is in agreement with the determinations made by the other methods.

3.4. Perturbation of the dephasing of the molecules at the crossing

Experimental studies were carried out of the nonresonant transitions described in Sect. 2.4 in which the static field ξ is set at the crossing value ξ_C. To understand the observed signals, the detection

Fig. 5. Normalized intensity due to the perturbation of the dephasing plotted as a function of the amplitude ε of the oscillating field causing the perturbation for (*a*) $\nu = 100$ kHz; (*b*) $\nu = 200$ kHz. The static electric field is set at the crossing value. The solid symbols are the experimental data. The lines were obtained by fitting the data to (17).

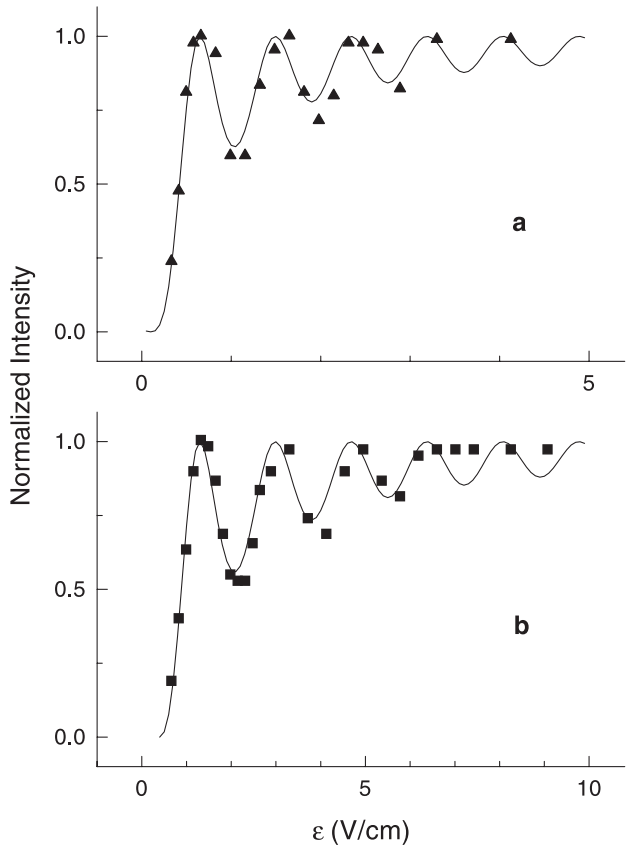

method must be examined in some detail. In the experiment, the amplitude ε of the oscillating field was square-wave-modulated on-off and a signal proportional to the number of molecules passing through the analyzer was obtained with a lock-in detector. As usual, the modulation period was long compared to the transit time τ of the molecules through the C-field. The detector signal is a measure of how many molecules are in state ($j = 1$) at the end of the C-field. During the half of the modulation cycle when the oscillating field is *off*, the molecules entering the C-field region follow the free decay (dephasing) discussed in Sect. 2.2, and the population of the ($j = 1$) state at the end of the C-field is given by $|\tilde{a}_1(\tau)|^2$; see (8). During the half of the modulation cycle when the oscillating field is *on*, the situation discussed in Sect. 2.4 applies and this population is given by $\left|a_1'(\tau)\right|^2$; see (17). The observed signal is proportional to the difference between these two populations, i.e., proportional to $\left|a_1'(\tau)\right|^2 - |\tilde{a}_1(\tau)|^2$. Thus, the observed signal results from the perturbation by the nonresonant oscillating field of the essentially resonant dephasing process that occurs when the oscillating field is off. Of course, since $|\tilde{a}_1(\tau)|^2$ is independent of ε, the detected signal will be determined by $\left|a_1'(\tau)\right|^2$ except for a constant which is of no interest under the experimental conditions used here.

Intensity measurements were carried out as a function of ε with the static field ξ set to the crossing value ξ_C. Data were taken first for $\nu = 100$ kHz and then for $\nu = 200$ kHz. In panels (*a*) and (*b*), respectively, of Fig. 5, these data are compared to the best fits obtained using (17). The only adjustable

parameters again were ν_c and the signal normalization. As was the case for the signals shown in Fig. 3, these free parameters do not affect the values of ε at which the intensity maxima occurred. The positions of these maxima are very insensitive to ν_c, and are largely determined by the maxima in the Bessel function $J_0[(\mu_{22} - \mu_{11})\,\varepsilon/\hbar\omega]$, whose argument is fixed once the experimental conditions are known. The observation of as many as three maxima for each value of ν and the agreement of the observed positions of the maxima with their theoretical counterparts were particularly satisfying. The best fit values obtained for ν_c were 2.9(8) and 3.2(8) kHz for panels (*a*) and (*b*), respectively, with a mean of 3.1(6) kHz. As was argued in Sect. 3.3, these values will be a little too small because the velocity spread in the molecular beam was not taken into account. Nonetheless, the value of ν_c still seems to be too low. However, given the 10 to 20% statistical errors typical in these determinations, the agreement is satisfactory.

4. Conclusion

A novel type of nonresonant absorption signals has been observed with molecular beam techniques in a two-level anticrossing system when the external static electric field ξ is at (or near) the crossing value ξ_C. These signals have been shown to arise from the ac Stark effect in systems where the energy of at least one of the levels has a linear dependence on the external electric field. When the two levels are at the crossing field and no oscillating electric field is applied, a dephasing occurs that can lead to a large transition probability. When an oscillating field is applied, a significant perturbation of the dephasing is produced that leads to the nonresonant signals detected. The dependence of the signal strength on the amplitude and frequency of the oscillating field has been studied, and shown to agree well with calculations based on this dephasing process. Because the signals are strong and nonresonant, they provide the basis for a sensitive, rapid-scan method of measuring the crossing field that is particularly useful when the initial uncertainty in the crossing value is large. While this method has been demonstrated only with the molecular beam method, it may well be useful in studies of avoided crossings with other techniques.

The oscillatory behaviour of the intensities as a function of the amplitude of the ac field provides the basis of a method for determining the magnitude ($\nu_c/2$) of the matrix element coupling the two levels undergoing the avoided crossing. The particular avoided crossing studied here is between the two levels[10] ($J = 1, K = \mp 1, \sigma = 0, m_J = \pm 1, \Gamma = E_1$) and ($1, \pm 1, \mp 1, \pm 1, E_3$) in CH_3SiH_3. In this case, there are in general three nuclear hyperfine interactions that can contribute to $\nu_c/2$: the spin–rotation Hamiltonian H^t_{sr} for the protons in the methyl top;[11] the dipole–dipole Hamiltonian H^t_{ss} for pairs of proton spins in the methyl top; and the corresponding interaction H^{tf}_{ss} between a proton in the methyl top and a proton in the silyl frame. It has been shown in ref. 13 that the matrix elements of H^t_{ss} are significantly larger than those of H^{tf}_{ss}, and so $\nu_c/2$ is expected to be due primarily to $H^t_{ss} + H^t_{sr}$. The mean value obtained here for $\nu_c/2$ is (2.3 ± 0.5) kHz. If $\nu_c/2$ were due only to H^t_{ss}, then this coupling matrix element would be 4.7 kHz, as was calculated from the molecular geometry and the proton g-factor [13]. Within the error, this is a factor of two larger than $\nu_c/2$, but this fact is believed to be accidental. It appears that the H^t_{sr} and H^t_{ss} contributions are approximately equal; however see also Sect. 4B of ref. 13 and Sect. 5.3 of ref. 11.

While the current measurements of $\nu_c/2$ have considerable scatter and their interpretation must be substantiated with further work, it is clear that the current method of measuring $\nu_c/2$ has the potential to provide a useful technique for studying these symmetry-breaking hyperfine interactions. When the minimum separation ν_c between the two interacting states is larger than the instrumental resolution,

[10] See footnote 4.

[11] It can be seen from Table XIII of ref. 13 that the spin–rotation Hamiltonian for the protons in the silyl frame cannot couple the two levels involved in the particular avoided crossing being discussed here.

the value of ν_c can be determined by frequency measurements. However, when ν_c is significantly smaller than the linewidth, this cannot be done. Under these circumstances, a procedure such as that developed here can be very useful. Similar molecular beam methods involving intensity studies have been demonstrated earlier, for example, in refs. 2 and 8.

References

1. D.R. Dion and J.O. Hirschfelder. Adv. Chem. Phys. **35**, 265 (1976).
2. W.L. Meerts, I. Ozier, and J.T. Hougen. J. Chem. Phys. **90**, 4681 (1989).
3. L. Martinache, I. Ozier, and A. Bauder. J. Chem. Phys. **92**, 7128 (1990); **94**, 831 (1991).
4. J. Margerie and J. Brossel. C.R. Acad. Sci. **241**, 373 (1955).
5. W.J. Meath, R.A. Thuraisingham, and M.A. Kmetic. Adv. Chem. Phys. **73**, 307 (1989).
6. R.C. Stoneman, D.S. Thompson, and T.F. Gallagher. Phys. Rev. A: Gen. Phys. **37**, 1527 (1988).
7. M. Gatzke, M.C. Baruch, R.B. Watkins, and T.F. Gallagher. Phys. Rev. A: At. Mol. Opt. Phys. **48**, 4742 (1993).
8. I. Ozier and W.L. Meerts. Can. J. Phys. **59**, 150 (1981).
9. W.L. Meerts and I. Ozier. J. Mol. Spectrosc. **94**, 38 (1982).
10. I. Ozier and W.L. Meerts. Can. J. Phys. **62**, 1844 (1984); **63**, 1375 (1985).
11. W.L. Meerts and I. Ozier. Chem. Phys. **71**, 401 (1982).
12. W.L. Meerts and I. Ozier. Phys. Rev. Lett. **41**, 1109 (1978).
13. J.T. Hougen, W.L. Meerts, and I. Ozier. J. Mol. Spectrosc. **146**, 8 (1991).
14. I. Ozier and W.L. Meerts. J. Mol. Spectrosc. **93**, 164 (1982).
15. K. Shimoda. Introduction to laser physics. 2nd ed. Springer, Berlin. 1986.
16. M. Abramowitz and I.A. Stegun. Handbook of mathematical functions. Dover, New York. 1955.
17. F.H. de Leeuw and A. Dymanus. J. Mol. Spectrosc. **48**, 427 (1973).
18. F.H. de Leeuw. Ph.D. thesis, Katholieke Universiteit, Nijmegen, The Netherlands. 1971.
19. W.L. Meerts and I. Ozier. J. Chem. Phys. **75**, 596 (1981).